
**International Journal of Abrasive Technology**

ISSN online: 1752-265X - ISSN print: 1752-2641
https://www.inderscience.com/ijat

# Study on cutting forces in zero-cutting after complete stop of feed motion when face milling of alloy 718

Shinpei Tanaka, Ryutaro Tanaka, Katsuhiko Sekiya, Keiji Yamada

**DOI:** 10.1504/IJAT.2023.10052374

**Article History:**

| | |
|---|---|
| Received: | 20 June 2022 |
| Accepted: | 05 October 2022 |
| Published online: | 12 May 2023 |

# Study on cutting forces in zero-cutting after complete stop of feed motion when face milling of alloy 718

Shinpei Tanaka, Ryutaro Tanaka*,
Katsuhiko Sekiya and Keiji Yamada

Graduate School of Advanced Science and Engineering,
Hiroshima University,
1-4-1 Kagamiyama, Higashi-Hiroshima, Hiroshima, 739-8527, Japan
Email: m211962@hiroshima-u.ac.jp
Email: ryu-tanaka@hiroshima-u.ac.jp
Email: sekiya@hiroshima-u.ac.jp
Email: keiji@hiroshima-u.ac.jp
*Corresponding author

**Abstract:** The cutting forces after the feed motion started to decelerate were investigated to establish a novel method to evaluate the friction characteristic between cutting tool and work material. The cutting force component in cutting direction *Ft* and that in the direction at right angle to cutting direction *Fn* decreased with the deceleration of feed speed and then showed almost constant in zero-cutting. In zero-cutting, the repeatability of wave form of cutting force was high and visually chips were not found. Because the contact was in the friction state without chip formation, the average cutting force rate *Ft′*/*Fn′* in zero-cutting could be defined as coefficient of friction. Therefore, a user can easily evaluate the friction characteristic of tool-work material and set appropriate cutting conditions. Comparing the average cutting force rate in zero-cutting of alloy 718, the emulsion 10% caused smaller average cutting force rate than dry condition.

**Keywords:** intermittent cutting; feed motion; uncut chip thickness; cutting force; zero-cutting; elastic deformation; friction characteristic; coefficient of friction.

**Reference** to this paper should be made as follows: Tanaka, S., Tanaka, R., Sekiya, K. and Yamada, K. (2023) 'Study on cutting forces in zero-cutting after complete stop of feed motion when face milling of alloy 718', *Int. J. Abrasive Technology*, Vol. 11, No. 3, pp.175–183.

**Biographical notes:** Shinpei Tanaka is a Master's course student at Graduate School of Advanced Science and Engineering, Hiroshima University, Japan. He graduated School of Engineering, Hiroshima University in 2021. His research interests focus on metal cutting process.

Ryutaro Tanaka is a Professor (Special Recognition) at Graduate School of Advanced Science and Engineering, Hiroshima University, Japan. His research interests focus on friction characteristic between cutting tool and work materials, cutting temperature, surface roughness and tool wear in cutting difficult-to-cut materials.

Katsuhiko Sekiya is an Assistant Professor at Graduate School of Advanced Science and Engineering, Hiroshima University, Japan. His research interests focus on tool wear, adhesion of work material and surface roughness in cutting difficult-to-cut materials.

Keiji Yamada is a Professor at Graduate School of Advanced Science and Engineering, Hiroshima University, Japan. His research interests focus on vibration analysis in cutting process, laser processing technology such as laser cleaving of brittle materials and laser dressing of diamond wheels.

This paper is a revised and expanded version of a paper entitled 'Cutting forces in zero-cutting after completely stop of feed motion when face milling of alloy 718' presented at the 24th International Symposium on Advances in Abrasive Technology, Guangdong University of Technology, 9–12 December 2022.

## 1 Introduction

To suppress tool wear and improve surface roughness, the tool materials and hard coatings of high wear resistance and adhesion resistance are utilised (Martinez et al., 2017; Okada et al., 2010). Especially in the cutting of difficult to cut materials, it's indispensable to supply cutting fluids to the contact area between cutting tool and work material (Nishimoto et al., 2012; Tanaka et al., 2015). Therefore, it will be possible to understand the cutting phenomenon more deeply and to optimise cutting conditions by making clear the friction characteristic among tool, work material, and cutting fluid. However, due to the complexity of cutting phenomenon, the findings obtained from cutting force itself are limited. For example, the lubricating effect of cutting fluids has the action to decreases cutting forces by preventing adhesion of a work material at the contact area between tool and work material. At the same time, the lubricating effect decrease cutting heat, as a result, the decreasing of deformation force at share plane by temperature rising is suppressed. The cooling effect of cutting fluids also suppresses decreasing of the deformation force. In some cases, the supply of cutting fluids increases the cutting force compared with dry cutting (Araki et al., 2017). Therefore, it is difficult to evaluate the friction characteristics between tool and work material even if it is possible to evaluate the effect of cutting fluids on cutting force. There are few standardised friction tests (Puls et al., 2014; Tortora and Veeregowda, 2016). Though these methods need a special testing equipment and a sample of special shape (Tortora and Veeregowda, 2016), it is difficult to realise both high temperature and high pressure such at the tool-work contact area in cutting.

By the way, the contact state between tool and work material immediately after the tool contacts with the work material in up-cut is in elastic deformation state. The elastic deformation state is in extremely brief time. Then, the contact state shifts to plastic deformation state and cutting state (Okamura et al., 1977; Uno and Tsuwa, 1976). The cutting force rate defined as principal force divided by thrust force in the elastic deformation state is stable and smaller than that in cutting state. The cutting force rate increases in plastic deformation state until cutting state and the rate is stable again in cutting state. The method to evaluate the friction characteristic using cutting forces in elastic deformation state in up-cut had already been proposed by some of authors

(Kitamura et al., 2020). However, it's difficult to distinguish the elastic deformation state from the other states. Especially in dry cutting, it's necessary to try many times. Like mentions above, the easily evaluation method to evaluate the friction characteristic between tool and work material for machining operator is not established yet. These methods are required in manufacturing industry.

In this study, the transition of cutting forces and the contact state among tool, work material and cutting fluids were investigated around the deceleration of feed motion to establish the easily on-the-machine method to evaluate the frictional characteristic among tool, work material and cutting fluids. This method focused on the phenomenon that the output of cutting forces was detected even after the feed motion stopped completely.

## 2 Experimental procedures

### *2.1 Experimental setup*

Figure 1 illustrates the schematic of experimental setup. The work material of alloy 718 was used in this study. The work material of width 17.5 mm was fixed on a piezoelectric dynamometer on the table of a milling machine. The diameter of end mill holder (KYOCERA MTES335) was 35 mm.

**Figure 1** Schematic of experimental setup (see online version for colours)

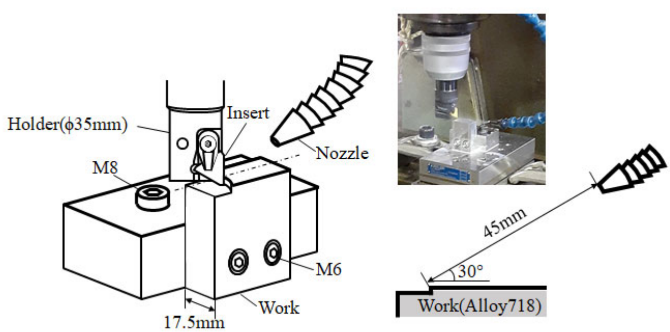


**Table 1** Cutting conditions

| | |
|---|---|
| Cutting speed | 73.1 [m/min] (665[rpm]) |
| Depth of cut | 1.0 [mm] |
| Feed | 32 [mm/min] |
| Work | Alloy718 (width 17.5 [mm]) |
| Tool holder | KYOCERA/MTE335 |
| Insert | Cemented carbide, MITSUBISHI MATERIALS/UTi20T/TEN1603PETR1/ |
| Cutting method | Face milling |
| Atmosphere | Dry, Emulsion10% mist lubrication |
| | (Idemitsu/Daphne alpha cool EX-1) [1.2L/h] |
| Machine tool | Universal milling machine, NIIGATA ENGINEERING/model 2UMC |

The cutting fluids were supplied by the mist supply method. The nozzle was set in the direction of centre line of a work material. The minimum distance between an insert and nozzle was approximately 45 mm.

Table 1 lists the cutting conditions. The used insert was an uncoated cemented carbide insert with an edge roundness of 4 μm (Mitsubishi Materials UTi20T, TEEN1603PETR1). The work material was a Ni-based superalloy alloy 718. The cutting was performed in dry condition and mist lubrication condition of emulsion 10%.

Figure 2 shows the motion of the cutting tool in one cutting process. The cutting tool fixed on spindle was rotated and fed in the positive direction of Z-axis until the axial depth of cut line. Afterwards, the tool was fed in the positive direction of Y-axis with rotating and stops feed motion after 20 times of cutting. Then, the spindle was fed in the negative direction of Z-axis after 10 s dwell time. The zero-cutting was performed during the dwell time.

**Figure 2** Motion of cutting tool in one cut pass process (see online version for colours)

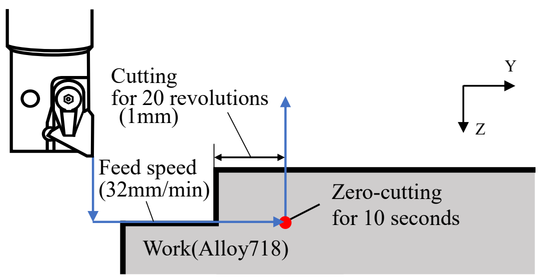


## 2.2 *Calculation of cutting forces in the coordinate system fixed on an insert*

Figure 3 shows the cutting forces applied to an insert. Cutting forces was measured in the $F_x$-$F_y$-$F_z$ coordinate system fixed on a tool dynamometer on the table. The forces measured in $F_x$-$F_y$-$F_z$ were transformed to the forces in $F_t$-$F_r$-$F_z$ coordinate system fixed on an insert as shown in equation (1). The tangential component to the tool rotation circle of cutting forces is defined as $F_t$. The radial component to the tool rotation circle of the cutting forces is defined as $F_r$. The resultant force of $F_z$ and $F_r$ was defined as $F_n$. These forces are shown in equation (1).

$$\begin{cases} F_t = Fx\sin\theta + Fy\cos\theta \\ F_r = -F_x\cos\theta + F_y\sin\theta \\ F_n = \sqrt{F_r^2 + F_z^2} \end{cases} \tag{1}$$

Because the axial rake of the used endmill was 15°, the actual cutting edges were located over a certain range of the angle $\theta$. Therefore, the angle $\theta$ at the first contact point was used as the representative position angle.

**Figure 3** Cutting forces applied to an insert (see online version for colours)

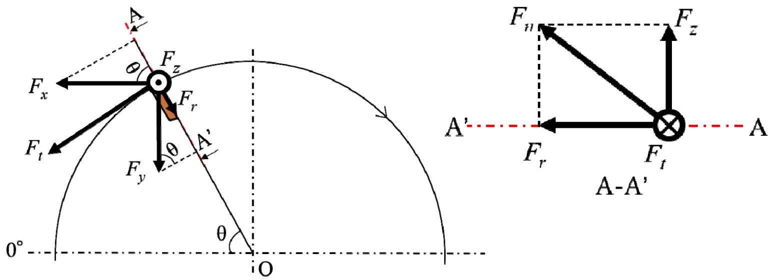


## 2.3 *Transition of uncut chip thickness with feed deceleration*

There must be the deceleration time from the feed speed starts to decrease to completely stop. Figure 4 shows the feed speed in deceleration time. The distance to an object on a table was measured with a laser displacement censor fixed on a spindle around the deceleration time. It was found that the deceleration time of used milling machine was 600ms at the feed rete of 32 mm/min.

**Figure 4** Feed speed in deceleration time (see online version for colours)

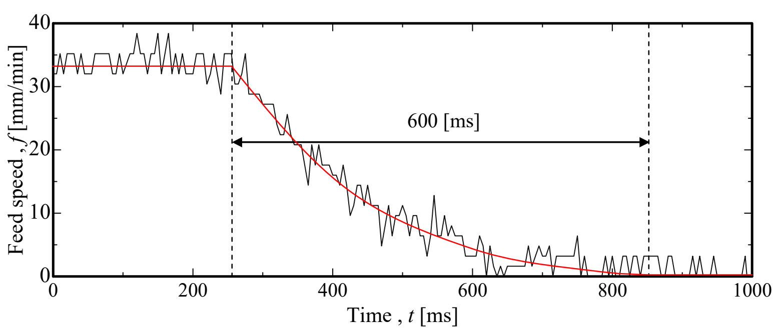


**Figure 5** Trajectory of tool edge around the completely stop of feed (see online version for colours)

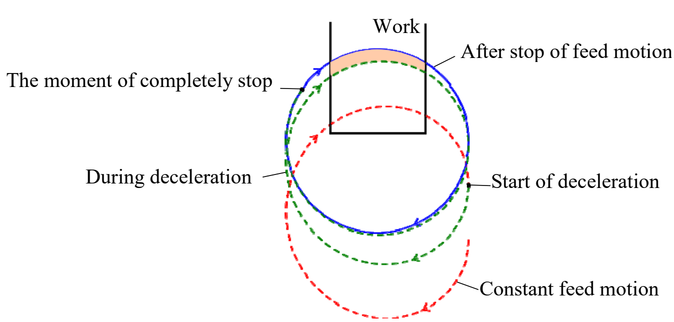

Figure 5 shows the trajectory of tool edge around the completely stop of feed. The feed speed assumed to decrease lineally. When the spindle is in feed motion with rotating, the trajectory of cutting edge of the tool top draws not a perfect circle but a trochoidal curve. The trajectory in feed motion is shown as the dotted line in the figure. The tool top draws perfect circle as the solid line after the completely stop of feed.

Therefore, the trajectories before and after the completely stop of feed motion does not consistent each other. Consequently, at least one cut pass occurs after the completely stop of feed motion in theoretically. Then, the uncut chip thickness becomes zero. The painted area indicates the uncut chip area in cutting just after the completely stop of feed motion.

Figure 6 shows the change in calculated uncut chip thickness around the completely stop of feed motion. The cutting pass after the feed speed starts to decrease were named $n = 1, 2, 3 \cdots$. It is found that uncut chip thickness does not show zero in waveform of $n = 7$ just after the completely stop of feed motion.

The zero-cutting where the calculated uncut chip thickness was zero starts at $n = 8$.

**Figure 6** Calculated uncut chip thickness with deceleration of feed

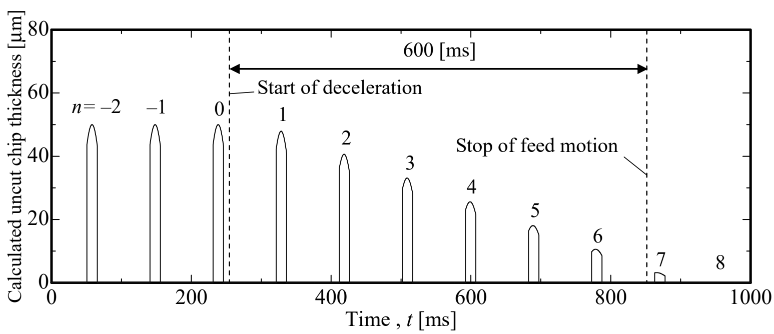


## 3 Results and consideration

Figure 7 shows the output of cutting force $F_y$ during one cut pass process.

When the feed rate was set at 32mm/min, the zero-cutting should start at $n = 8$. The cutting force $F_y$ were almost constant after waveform of $n = 8$ where the calculated uncut chip thickness became zero.

Figure 8 shows the cutting forces and the rate of cutting forces $F_t/F_n$ during one cut pass at the feed rate of 32 mm/min. The start of one cut pass was defined as the moment when the cutting force $F_n$ started to increase. The end of cutting can be calculated from rake angle, axial depth of cut and cutting speed. When the feed rate was kept at constant, the forces, $F_t$ and $F_n$ stably showed approximately 600 N and 350 N, respectively. The cutting force rate $F_t/F_n$ was kept at approximately 0.6 during one cut pass. Note that the rate $F_t/F_n$ was influenced by the force which generated chip at share zone.

Figure 9 shows the cutting forces and the cutting force rate $F_t/F_n$ during one cut pass after the completely stop of feed motion. Any cutting forces were smaller than those at the constant feed rate. However, the cutting forces were unstable around both start and end of cutting due to axial rake. Therefore, the initial 10% and latest 10% of cutting time were excepted from the evaluation target. It was found that the forces $F_n$ and $F_t$ were stable during one cut pass around 400 N and 150 N, respectively. The cutting force rate $F_t/F_n$ was also stable at around 0.4. The average cutting forces, $F_t'$ and $F_n'$ during one cut pass was defined as equation (2).

$$F_t' = \frac{1}{t_0}\int_0^{t_0} F_t(t)\mathrm{d}t \quad F_n' = \frac{1}{t_0}\int_0^{t_0} F_n(t)\mathrm{d}t \tag{2}$$

The average cutting force rate $F_t'/F_n'$ was defined as the representative evaluation value for contact state.

**Figure 7** Output of cutting force $F_y$ during one cut pass process

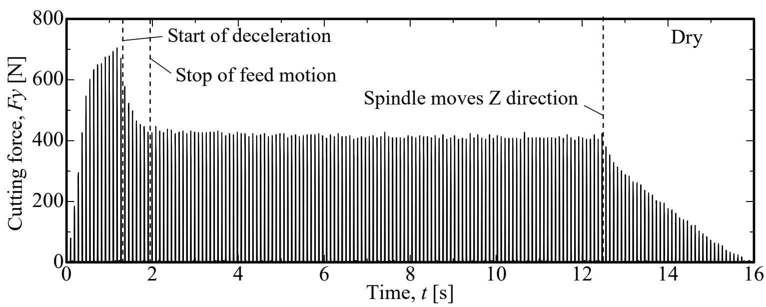


**Figure 8** Cutting forces and friction characteristic for one cut pass at the constant feed rate, (a) cutting force $F_x$, $F_y$, $F_z$, (b) cutting force $F_t$, $F_n$ and cutting force rate $F_t/F_n$ (see online version for colours)

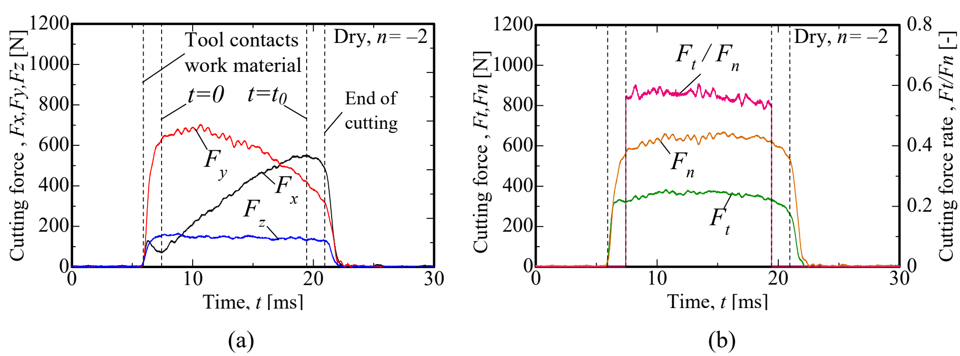


Figure 10 shows the transition of average cutting force rate after the feed motion starts to decelerate. After the feed motion start to decelerate, the average cutting force rate also decreased and was stable after the completely stop of feed motion. Comparing the average cutting force rate around the completely stop of feed motion, the emulsion 10% caused smaller average cutting force rate than dry condition. This tendency was like the transition of the measured feed speed shown in Figure 4. The decelerating of feed speed decreased the uncut chip thickness. Consequently, the cutting force decreased.

As shown in Figure 6, zero-cutting was occurred after the completely stop of feed motion, where the plastic deformation and elastic deformation of work material might occur, but the visible chip was not formed. In addition, the cutting force rate during one cut pass showed stable. Therefore, the contact state was thought to be kept constant during one cut pass. The average cutting force rate $F_t'/F_n'$ could be defined as coefficient of friction especially after the completely stop of feed motion. The proposed method made it easy to evaluate the frictional characteristic between tool and work material because the problem that the elastic deformation state in up-cut is too brief to distinguish from the other contact states could be avoid. Therefore, using this method, users of cutting tools and cutting fluids can easily evaluate the friction characteristic of them by themselves and set appropriate cutting conditions.

**Figure 9** Cutting forces and cutting force rate for one cut pass after the completely stop of feed motion, (a) cutting force $F_x$, $F_y$, $F_z$, (b) cutting force $F_t$, $F_n$ and cutting force rate $F_t/F_n$ (see online version for colours)

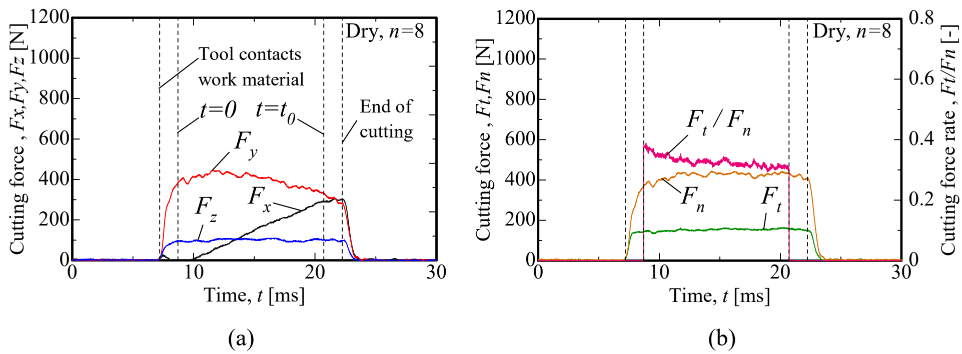


**Figure 10** Transition of average cutting force rate after the feed motion starts to decelerate (see online version for colours)

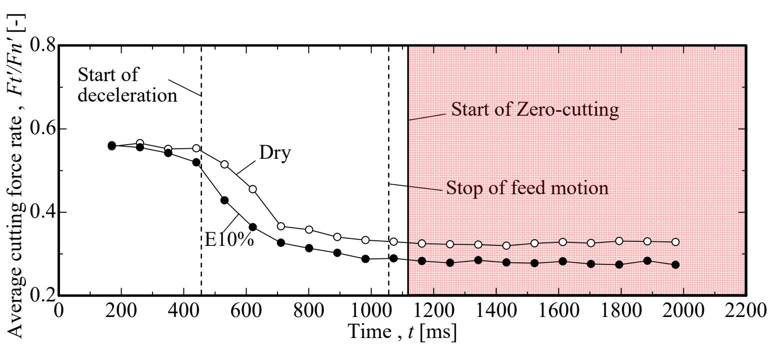


## 4 Conclusions

In this study, the transition of cutting force and the contact state among tool, work material and cutting fluids were investigated after the feed speed started to decelerate. The results obtained in this study were as follows:

1 The output of cutting force could be observed even after the completely stop of feed motion. The force was smaller than that at the constant feed rate, but their repeatability was high.

2 The tendency of measured feed speed was consistent with that of cutting force rate after the feed speed started to decelerate. At least one cut pass occurs after the completely stop of feed motion in theoretically. Zero-cutting was occurred after the one cut pass after the completely stop of feed motion, where the visible chip was not formed.

3 Comparing the average cutting force rate around the completely stop of feed motion, the emulsion 10% caused smaller average cutting force rate than dry condition.

## Acknowledgements

The authors wish to acknowledge the financial support provided by the Grant-in-Aid for Scientific Research(C) 22K03885, Japan.

## References

Araki, Y., Tanaka, R., Kojima, Y., Sekiya, K., Yamada, K. and Koseki, S. (2017) 'Relationship between cutting heat and tool edge temperature in end milling of titanium alloy', *Key Engineering Materials*, Vol. 749, pp.15–20.

Kitamura, T., Tanaka, R., Yamane, Y., Sekiya, K. and Yamada, K. (2020) 'Performance evaluation method for cutting fluids using cutting force in micro-feed end milling', *Precision Engineering*, Vol. 62, pp.232–243.

Martinez, I., Tanaka, R., Yamane, Y., Sekiya, K., Yamada, K., Ishihara, T. and Furuya, S. (2017) 'Wear mechanism of coated tools in the turning of ductile cast iron having wide range of tensile strength', *Precision Engineering*, Vol. 47, pp.46–53, available online 2016-7-16.

Nishimoto, H., Tanaka, R., Hosokawa, A., Ueda, T. and Furumoto, T. (2012) 'Development of tool edge temperature measurement method in wet cutting (application for CBN and poly crystalline diamond tools)', *Journal of Advanced Mechanical Design, Systems, and Manufacturing*, Vol. 6, No. 6, pp.916–922.

Okada, M., Hosokawa, A., Tanaka, R. and Ueda, T. (2010) 'Cutting performance of PVD-coated carbide and CBN tools in hardmilling', *International Journal of Machine Tools and Manufacture*, Vol. 51, No. 2, pp.127–132.

Okamura, K., Nakajima, T. and Uno, Y. (1977) 'Study on the transitional cutting process (2nd report) – analysis of surface generation mechanism in up milling', *Journal of the Japan Society of Precision Engineering*, Vol. 43, No. 509, pp.597–602.

Puls, H., Klocke, F. and Lung, D. (2014) 'Experimental investigation on friction under metal cutting conditions', *Wear*, Vol. 310, Nos. 1–2, pp.63–71.

Tanaka, R., Hosokawa, A., Furumoto, T., Okada, M. and Ueda, T. (2015) 'Influence of cutting fluid on tool edge temperature in end milling titanium alloy', *Journal of Advanced Mechanical Design, Systems, and Manufacturing*, Paper No. 14-00509, Vol. 9, No. 5, p.JAMDSM0074.

Tortora, A.M. and Veeregowda, D.H. (2016) 'True stability of lubricants determined using the ball-on-disk test', *Advances in Tribology*, Vol. 2016, Article ID 4020537.

Uno, Y. and Tsuwa, H. (1976) 'Study on the transitional cutting process (1st report) – transient phenomena in the initial part of contact between tool and workpiece', *Journal of the Japan Society of Precision Engineering*, Vol. 42, No. 496, pp.358–363.